

RESEARCH ARTICLE

Quantitative spatial analysis reveals that the local axons of lamina I projection neurons and interneurons exhibit distributions that predict distinct roles in spinal sensory processing

Éva Kókai^{1,2} | Lilana L. Luz^{3,4} | Elisabete C. Fernandes^{3,4} | Boris V. Safronov^{3,4} | Pierrick Poisbeau⁵ | Peter Szucs^{1,2} 

¹Department of Anatomy, Histology and Embryology, Faculty of Medicine, University of Debrecen, Debrecen, Hungary

²ELKH-DE Neuroscience Research Group, Debrecen, Hungary

³Instituto de Investigação e Inovação em Saúde, Universidade do Porto, Porto, Portugal

⁴Neuronal Networks Group, Instituto de Biologia Molecular e Celular (IBMC), Universidade do Porto, Porto, Portugal

⁵Centre national de la Recherche Scientifique, Institut des Neurosciences Cellulaires et Intégratives, University de Strasbourg, Strasbourg, France

Correspondence

Peter Szucs, Department of Anatomy, Histology and Embryology, Faculty of Medicine, University of Debrecen, Nagyerdei krt. 98., 4032 Debrecen, Hungary.
Email: szucs.peter@med.unideb.hu

Funding information

FEDER—Fundo Europeu de Desenvolvimento Regional funds through the COMPETE 2020—Operacional Programme for Competitiveness and Internationalization (POCI), Portugal 2020, Grant/Award Number: POCI-01-0145-FEDER-016588; Hungarian Brain Research Program, Grant/Award Numbers: KTIA_NAP_13-2-2014-0005, 2017-1.2.1-NKP-2017-00002; Marie-Curie Short Term Fellowship; Graduate School of Pain (EURIDOL); French National Research Agency - ANR, Grant/Award Number: ANR-17-EURE-022; FCT—Fundação para a Ciência e a Tecnologia/Ministério da Ciência, Tecnologia e Ensino Superior, Grant/Award Numbers: PTDC/NEU-NMC/1259/2014, SFRH/BPD/120097/2016, SFRH/BD/118129/2016

Abstract

Our knowledge about the detailed wiring of neuronal circuits in the spinal dorsal horn (DH), where initial sensory processing takes place, is still very sparse. While a substantial amount of data is available on the somatodendritic morphology of DH neurons, the laminar and segmental distribution patterns and consequential function of individual axons are much less characterized. In the present study, we fully reconstructed the axonal and dendritic processes of 10 projection neurons (PNs) and 15 interneurons (INs) in lamina I of the rat, to reveal quantitative differences in their distribution. We also performed whole-cell patch-clamp recordings to test the predicted function of certain axon collaterals. In line with our earlier qualitative description, we found that lamina I INs in the lateral aspect of the superficial DH send axon collaterals toward the medial part and occupy mostly laminae I–III, providing anatomical basis for a lateromedial flow of information within the DH. Local axon collaterals of PNs were more extensively distributed including dorsal commissural axon collaterals that might refer to those reported earlier linking the lateral aspect of the left and right DHs. PN collaterals dominated the dorsolateral funiculus and laminae IV–VI, suggesting propriospinal and ventral connections. Indeed, patch-clamp recordings confirmed the existence of a dorsoventral excitatory drive upon activation of neurokinin-1 receptors that, although being expressed in various lamina I neurons, are specifically enriched in PNs. In summary, lamina I PNs and INs have almost identical dendritic input fields, while their

This is an open access article under the terms of the [Creative Commons Attribution-NonCommercial-NoDerivs](https://creativecommons.org/licenses/by-nc-nd/4.0/) License, which permits use and distribution in any medium, provided the original work is properly cited, the use is non-commercial and no modifications or adaptations are made.

© 2022 The Authors. *The Journal of Comparative Neurology* published by Wiley Periodicals LLC.

segmental axon collateral distribution patterns are distinct. INs, whose somata reside in lamina I, establish local connections, may show asymmetry, and contribute to bridging the medial and lateral halves of the DH. PNs, on the other hand, preferably relay their integrated dendritic input to deeper laminae of the spinal gray matter where it might be linked to other ascending pathways or the premotor network, resulting in a putative direct contribution to the nociceptive withdrawal reflex.

KEYWORDS

dorsoventral excitatory drive, laminar axon density, mediolateral asymmetry, quantitative analysis, withdrawal reflex

1 | INTRODUCTION

Sensory information from somatic and visceral primary afferents is received and processed by complex dorsal horn (DH) neuronal circuits, formed by local and propriospinal interneurons (INs) and projection neurons (PNs) as output elements, eventually transmitting the information to supraspinal targets (Todd, 2010).

Primary afferent termination patterns have been intensively studied and different sensory modalities have been shown to terminate in a strict order (Brown, 1981; Fitzgerald, 1989; Fyffe, 1984; Ramon y Cajal, 1909; Rethelyi, 1984; Todd, 2010). This fact along with the special spatial constraints of the elongated and segmented spinal cord suggested that dendritic trees of second-order neurons should be specifically shaped for receiving input from the relevant primary afferents. Indeed, using the Golgi method, Ramon y Cajal (1909) described various types of neurons that later were categorized into different groups, mostly on the basis of their distinct dendritic trees and soma location within the spinal DH (Brown, 1981; Schoenen, 1982; Todd, 2010) but rarely taking the axonal arbors into consideration (Gobel, 1978). The use of transgenic mice and the vast array of emerging anatomical (Gatto et al., 2019; Todd, 2017), imaging (Kosugi et al., 2013), and tracing methods (Gutierrez-Mecinas et al., 2018) along with single cell electrophysiology (Lu & Perl, 2005; Santos et al., 2007; Yasaka et al., 2010) and transcriptional profiling (Haring et al., 2018) helped to identify various classes of excitatory and inhibitory neurons with specific laminar locations. Yet, few studies described detailed axon morphology of the identified cell groups (Yasaka et al., 2010). Although single-cell electrophysiology and recordings from synaptically connected neurons (Lu & Perl, 2003, 2005; Zheng et al., 2010), combined with optogenetic stimulation techniques (Duan et al., 2014; Gradwell et al., 2022; Smith et al., 2019), revealed detailed anatomical features and identified postsynaptic targets of certain specific cell types, these studies did not aim to reveal the distribution of the axon of individual neurons.

Lamina I or marginal zone, described as a “thin veil of gray matter” (Rexed, 1952), is one of the most difficult regions for single-cell labeling studies within the superficial DH. Early investigators regarded this lamina as the superficial part of the substantia gelatinosa (Ramon y Cajal, 1909; Ranson, 1913), but it is now clear that lamina I is a

separate structural and functional entity (Cervero & Iggo, 1980). The generally accepted classification schemes of lamina I neuron today differentiate either three or four subtypes: fusiform, multipolar, and pyramidal (Zhang & Craig, 1997; Zhang et al., 1996) or fusiform, multipolar, pyramidal, and flattened (Lima, 1998; Lima & Coimbra, 1986; Yu et al., 1999). These schemes may, however, reflect a continuum and are only based on somatodendritic features of the cells, ignoring axonal morphology or trajectory as a factor in the classification, since the use of the Golgi method did not reveal full axonal arbors reliably (Lima & Coimbra, 1986). Similarly, single-cell labeling methods either fail to give sufficient detail (e.g., retrograde tracers) or the standard slice preparation significantly limits the recovery of the processes. The existing detailed axonal reconstructions come from the early *in vivo* horseradish peroxidase (HRP) labeling studies in monkey and cat (Beal et al., 1981; Bennett et al., 1981) and the recent whole-cell patch-clamp experiments in whole spinal cords of rats (Szucs et al., 2010, 2013) and in mice (Browne et al., 2021). So, while the increasing use of transgenic mice (Gatto et al., 2019) led to the discovery of several neuronal circuits, formed by INs in deeper laminae and targeting lamina I PNs, there is very little morphological data that would allow placing lamina I INs and PNs themselves, via their axon collaterals, into these circuits (Browne et al., 2020). Furthermore, recent studies using laser-scanning photostimulation (Kosugi et al., 2013) and voltage-sensitive dye imaging (Mizuno et al., 2019) investigating lamina I neurons at a population level suggested that certain asymmetries that are likely based on morphological features of lamina I neurons contribute to spatial organization of information flow in the DH. Based on our earlier qualitative description of lamina I neuron axons (Szucs et al., 2010, 2013), our hypothesis was that there are quantitative differences in the amount of IN and PN axon collaterals in different superficial DH laminae and that these distinct patterns explain the abovementioned observations.

Thus, in the present work, we performed quantitative morphological analyses of individual lamina I neurons that were labeled in semi-intact spinal cord blocks of young rats. Putative PNs and INs, identified on the basis of the presence and absence, respectively, of a main axon projecting to the contralateral white matter, were reconstructed from transverse sections. This way, we aimed to correctly identify the laminar location of putative target cell populations and

wiring schemes of circuits involving lamina I neurons as information providers.

2 | MATERIALS AND METHODS

All cells analyzed in this work have been labeled in semi-intact spinal cord block preparations during whole-cell patch-clamp recording sessions in two sets of experiments that aimed to qualitatively describe the morphology and connectivity of lamina I PNs and INs (Luz et al., 2010; Szucs et al., 2010, 2013). We checked all 271 recovered neurons from these works to select the ones suitable for the present analyses. Suitable cells had to be (1) from sections in the transverse plane; (2) labeled in excellent detail; and (3) located in serial sections that were not distorted or damaged significantly. All of these conditions were met in 25 cases (9.2%).

2.1 | Preparation of lumbar spinal cord blocks

Details of the procedure are described in Szucs et al. (2010). Briefly, laboratory Wistar rats (P9–P20) were killed in accordance with the national guidelines (Direção Geral de Alimentação e Veterinária, Ministério da Agricultura) after anesthesia by intraperitoneal injection of Na⁺-pentobarbital (30 mg/kg) and subsequent check for lack of pedal withdrawal reflexes.

The vertebral column was quickly excised and transferred into oxygenated artificial cerebrospinal fluid (ACSF) at room temperature. The lumbar enlargement (segments L1–L6) of the spinal cord was dissected and either kept as a whole or cut into three pieces (L1–L2, L3–L4, and L5–L6) before the recording to minimize the overlap between the labeled neuronal processes. Thus, in the latter case, the full rostrocaudal extent of the processes could not be determined when the labeled neuron showed clear signs of truncation at the end of the preparation. The pia mater was locally removed along the lateral part of the dorsal surface on one side to provide access for the recording pipettes.

Recordings from lamina I neurons were performed in the most superficial layer of the spinal cord surface using the oblique IR-LED illumination technique (Szucs et al., 2009).

2.2 | Preparation of lumbar spinal cord slices

Laboratory Wistar rats (P6–P15) were killed under general anesthesia after intraperitoneal injection of Na⁺-pentobarbital (30 mg/kg) and subsequent check for lack of pedal withdrawal reflexes.

The vertebral column (thoracic and lumbar segments) was quickly excised and transferred into a chamber filled with ice cold oxygenated ACSF. Next, a 50-ml syringe filled with ACSF was inserted into a cut performed just above the sacrum and the spinal cord was flushed out into the chamber. The lumbar enlargement (segments L1–L6) of the spinal cord was cut out and the pia mater was carefully removed using two forcipies. This block was then glued to the stage of a vibrating tissue slicer (Leica VT1000) with an agar block matrix to support it during

the slicing procedure. Transverse 300- to 400-micron-thick slices were prepared and stored in a chamber filled with oxygenated ACSF at room temperature until their transfer into the recording chamber. In some experiments, the DH (laminae I–VI) with the surrounding white matter was separated from the rest of the spinal cord on one side, by using a 26-G needle.

2.3 | Whole-cell patch-clamp recording in spinal cord blocks and slices

Cells used for morphological analysis in this study were all labeled during whole-cell recordings performed in intact (i.e., nonsliced) lumbar spinal cord blocks. Details of the procedures are described in our previous works (Fernandes et al., 2018; Szucs et al., 2013). Briefly, ACSF contained (in mM) NaCl 115, KCl 3, CaCl₂ 2, MgCl₂ 1, NaH₂PO₄ 1, NaHCO₃ 25, and glucose 11 (bubbled with 95% O₂/5% CO₂). The pipettes were pulled from thick-walled glass (BioMedical Instruments, Germany) and fire polished (resistance, 4–5 MΩ). The pipette solution contained (in mM) KCl 3, K-gluconate 150, MgCl₂ 1, BAPTA 1, HEPES 10 (pH 7.3 adjusted with KOH, final [K⁺] was 160 mM), and 1% biocytin (Sigma). In some cases (*n* = 12), concentration of biocytin was reduced to 0.5% and it was complemented by 0.5% rhodamine red to help faster identification of the neuronal soma after serial sectioning.

Electrophysiological recordings aiming to test the hypothesis of the dorsoventral spread of excitation were carried out on spinal cord slices. In these experiments, the artificial cerebrospinal fluid contained (in mM) NaCl 126, KCl 3, CaCl₂ 2, MgCl₂ 2, NaH₂PO₄ 1.3, NaHCO₃ 26, and glucose 10 (bubbled with 95% O₂/5% CO₂). The pipettes were pulled from thick-walled glass (resistance, 3–5 MΩ). The whole cell recordings in spinal cord slices aimed to record often small, subthreshold postsynaptic potentials; thus, we used an intracellular solution that tried to be as close as possible to intracellular physiological ionic concentrations. The pipette solution contained (in mM) K-gluconate 124, NaCl₂ 14, ATP-Mg 1, GTP-Na 0.3, HEPES 10 (pH 7.3 adjusted with KOH), and 1% biocytin (Sigma).

Recordings were performed at room temperature and all drugs were applied in the bath with the use of a peristaltic pump (1.5–2 ml/min). Drugs used to test neuronal responses to substance P (SP) were SP (Sigma); SR140333 (Sanofi), a selective neurokinin 1 (NK1) receptor antagonist (Oury-Donat et al., 1994); [Sar9, Met(O2)11]-SP (Sigma), a selective NK1 receptor agonist; and TTX (Sigma). Repeated application of substance P was preceded by a 7- to 10-minute wash with normal ACSF. Recorded data were digitized by a Digidata 1320 A/D board, filtered at 5 kHz, and analyzed using Clampfit 8.0, Origin (Microcal Software, Northampton, MA, USA), Whole Cell Program, and Electrophysiology Data Recorder (Dr. J. Dempster, University of Strathclyde, Glasgow, UK).

Excitatory postsynaptic potentials (EPSPs) were detected offline. Control conditions were compared with the effect of the investigated drugs by determining an average EPSP number per second for a 120-s period at the beginning of the recording (control) and at the end of the drug application (effect).

2.4 | Histological processing

After fixation in 4% paraformaldehyde, the spinal cord was embedded in agar and transverse 100- μm -thick serial sections were cut with a vibrating tissue slicer (Leica VT1000). Transverse sections were used instead of sagittal ones to allow precise delineation of the laminae and measurement of exact mediolateral extent of the processes.

Spinal cord slices were immersed in 4% paraformaldehyde after the recording session. Fixed slices were flat re-embedded in agar and re-sectioned to 60- μm -thick sections.

To reveal biocytin, in both cases, sections were permeabilized with 50% ethanol and treated according to the avidin-biotinylated HRP method (ExtrAvidin-Peroxidase, Sigma, diluted 1:1000) followed by a diaminobenzidine chromogen reaction. To allow determination of the laminae and confirmation of the location of the recorded neuron in the intermediate gray matter, sections were counterstained with toluidine blue and mounted in DPX (Fluka).

2.5 | Cell reconstruction

3D reconstructions of lamina I neurons, filled in isolated spinal cord blocks, were done using NeuroLucida (versions 10 and 9; MBF Bioscience, Williston, USA). Each serial section (4–27 sections/neuron) with all its neuronal processes (dendrites and axons with varicosities) was traced in a separate serial section layer in NeuroLucida, using a 100 \times oil immersion objective. Certain landmarks (cracks, capillaries, etc.) were also labeled at lower magnification (10 \times objective) for correct alignment of the sections. Consecutive serial sections have been aligned by rotating them to find the best fit of the traced contours of the gray matter and section outlines. Each section was aligned to its neighbor proximal to the soma-containing section. The alignment procedure always started from the section containing the soma and sections were gradually aligned toward the rostral and caudal directions.

Dendrites and axons were identified as described earlier (Szucs et al., 2010, 2013); dendrites showed gradual tapering, usually dichotomic branching, and occasional spines. Axons, on the other hand, had an even diameter, branched frequently, often in angles close to perpendicular and possessed numerous varicosities of varying diameter (0.5–1.5 μm). In contrast to our earlier reconstructions from sagittal sections (Szucs et al., 2013), we did not aim to connect the continuing processes to form a single axonal or dendritic tree since, due to the plane of sectioning, the complex arbors (especially in case of lamina I IN axons) were cut in too many pieces. Note that none of the analyses performed in this work required a single connected tree.

2.6 | Quantification of total process lengths

Closed bounding contour lines have been delineated to measure the sum of the lengths of dendritic and axonal processes using the algorithm provided by NeuroLucida Explorer (versions 10 and 9; MBF Bioscience, Williston, USA). Laminal borders of adult rats could not be applied in our sections due to the age of our experimental animals.

Therefore, we determined eight regions for the spatial distribution analysis as follows. Toluidine blue background staining clearly outlined lamina II (substantia gelatinosa), whereas the region dorsal to it and within the gray matter was considered to be lamina I. Laminae III–IV were separated from laminae V–VI with a curved line resembling the same border in adult rats (Paxinos, 2007), starting from the innermost point on the lateral side of the neck of the DH and reaching the midpoint between the lower border of lamina II and the level of the lowermost point of the dorsal column. Laminae VII–X contained the rest of the gray matter below the lowermost point of the dorsal column. The white matter was divided into dorsal, lateral, and ventral parts separated by the ventral rootlets leaving and dorsal rootlets entering the spinal gray matter.

When determining the symmetry of axonal and dendritic trees, the following methods were used: For mediolateral symmetry measurements, a line perpendicular to the dorsal contour of the spinal DH and passing through the cell body has been drawn. This line served as a guide throughout the aligned serial sections and the ipsilateral spinal cord half has been split into a medial and lateral part along this line in all serial sections. Processes within the medial part were considered as being located medial to the cell body, while the ones falling in the lateral part were considered as lateral to it (graphical explanation in Figure 2a). To separate the processes along the rostrocaudal axis, serial sections of a given cell have been split into rostral and caudal groups starting from the section containing the soma. The section with the soma has been filtered in the Z-axis at the level where the soma contour was the largest. Processes rostral to this level have been cut and pasted into the rostral group of the split serial reconstruction, while caudal parts have been added to the caudal serial section group (Figure 2b). Process lengths in the two groups formed from the serial sections have been quantified separately.

When determining the distribution of processes between the medial and lateral parts of the DH, the area of laminae I–IV has been split into a medial and lateral half separated by a vertical line, perpendicular to the midpoint of the mediolateral extent of the dorsal contour of the gray matter.

2.7 | Statistics

Data are presented as “mean \pm SEM.” Statistical analyses were carried out using Origin 9 (Microcal Software, Northampton, MA, USA). Mediolateral and rostrocaudal symmetry comparisons were done using one-way ANOVA. Interlaminar differences were assessed with Mann–Whitney test, while EPSP frequency in control and during drug application periods was compared using the two sample Student's t-test with Welch correction.

3 | RESULTS

We performed complete reconstruction of 10 PNs and 15 INs that were filled intracellularly in lamina I of the spinal DH of young rats. Putative PNs and INs were distinguished based on the presence and

TABLE 1 Basic anatomical parameters and firing patterns of the neurons in this study

	Cell no.	Somatodendritic morphology (Lima & Coimbra, 1986)	Type of collaterals (Szucs et al., 2010)	Firing pattern (Luz et al., 2014)	Axon origin	Number of stem dendrites	More than 50% of dendrites located in LF
PNs	1	Flattened	Lateral	Tonic	Dendrite	4	No
	2	Flattened	Mixed	Tonic	Soma	4	No
	3	Flattened	Mixed	Tonic	Soma	5	Yes
	4	Multipolar	Lateral	Tonic	Dendrite	5	No
	5	Flattened	Ventral	Tonic	Soma	2	Yes
	6	Multipolar	Mixed	Tonic	Soma	5	No
	7	Multipolar	Lateral	Tonic	Dendrite	4	Yes
	8	Multipolar	Mixed	Tonic	Dendrite	4	No
	9	Pyramidal	Ventral	n.d.	Soma	4	No
	10	Flattened	No collateral	n.d.	Dendrite	4	No
INs	1	Multipolar		Tonic	Soma	5	No
	2	Multipolar		Tonic	Dendrite	7	No
	3	Multipolar		Rhythmic	Dendrite	7	Yes
	4	Multipolar		Rhythmic	Dendrite	4	Yes
	5	Flattened		Tonic	Soma	4	Yes
	6	Flattened		n.d.	Dendrite	4	No
	7	Multipolar		Rhythmic	Dendrite	6	No
	8	Multipolar		Rhythmic	Soma	7	No
	9	Multipolar		n.d.	Dendrite	8	Yes
	10	Multipolar		Tonic	Dendrite	7	No
	11	Multipolar		Tonic	Soma	6	Yes
	12	Fusiform		Gap	Soma	5	No
	13	Multipolar		Rhythmic	Soma	6	No
	14	Multipolar		Tonic	Soma	6	No
	15	Multipolar		Gap	Dendrite	5	No

absence, respectively, of a thick main axon crossing the midline in the anterior commissure and entering the contralateral anterolateral white matter. All 25 cells could be classified based on the somatodendritic classification of Lima and Coimbra (1986) and most had firing patterns reported earlier in lamina I (Table 1). Although the reconstructions of PNs contained the main axon, the quantitative analyses were performed only for its local spinal axon collaterals. One of the PNs did not have any local axon collaterals and was only used in the analyses of dendritic tree. The main axon of all PNs could clearly be traced to the contralateral white matter except one, which got gradually fainter and could not be followed beyond the level of the central canal. Nevertheless, the course and appearance of this main axon showed all the characteristics described earlier for PN main axons (Szucs et al., 2010). The mean total length of dendritic segments of PNs and INs was $4022 \pm 574 \mu\text{m}$ and $3215 \pm 373 \mu\text{m}$, respectively, while mean total axon length was $4697 \pm 1490 \mu\text{m}$ for PNs and $22,888 \pm 3211 \mu\text{m}$ for INs. These values, along with the number of stem dendrites in the two groups, showed the same difference and were comparable to those obtained from our complete connected 3D reconstructions of PNs and

INs from sagittal slices (Szucs et al., 2010, 2013). However, it should be noted that axons of 17 out of these 25 neurons reached one or the other end of the preparation; thus, the total length of the axon in these cases was underestimated.

3.1 | Branching patterns

Neuronal cell bodies reconstructed in this study were mostly located in the lateral half of the DH, due to the better accessibility of this region when using the intact spinal dorsal cord preparation. The transverse sectioning plane allowed better tracing of the fine collaterals running in the mediolateral direction. As a result of this, besides the regular PN collateral types (Figure 1a,b), we recovered collaterals that crossed the midline and invaded the contralateral gray matter. One of these PNs had a fine collateral branch that crossed the midline in the dorsal commissure and started ascending toward dorsal laminae before it got faint beyond being traceable (Figure 1c). This cell could have been classified as a ventral-collateral-type PN based on our earlier classification scheme (Szucs et al., 2010). Another mixed-collateral-type PN

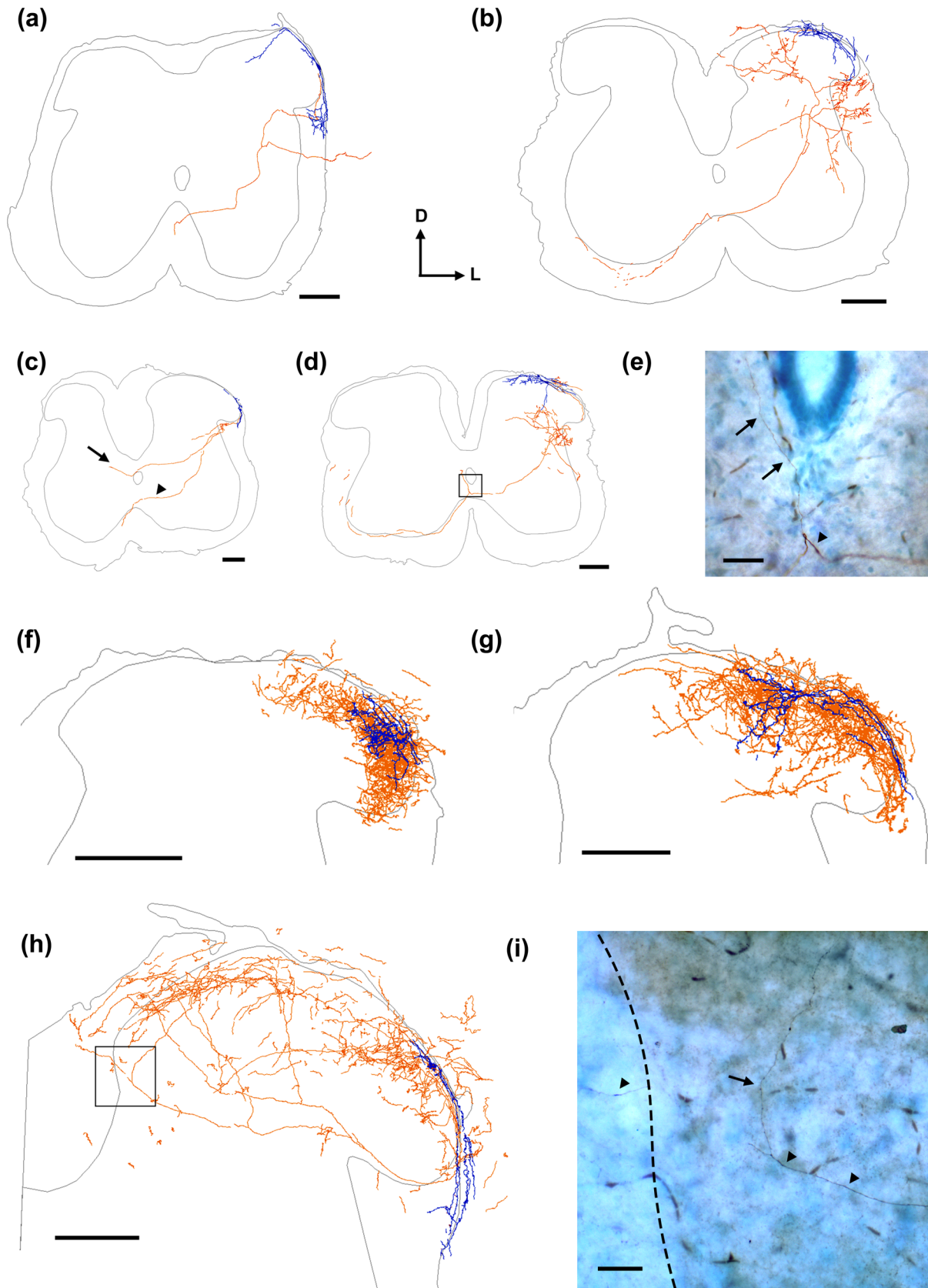


FIGURE 1 Representative examples of PN and IN axons. NeuroLucida reconstructions allowing comparison of the density of collaterals in a lateral-collateral-type (a) and a mixed-collateral-type PN (b). Note that the majority of collaterals target laminae deeper than lamina II. (c, d) Two

(Continues)

FIGURE 1 (Continued)

examples for novel types of commissural PN axon collaterals. (c) Ventrally oriented axon collateral branching from the main axon on the ipsilateral side and crossing the midline in the dorsal gray commissure through lamina X. (d) Collateral branching on the contralateral side from the main axon after crossing the midline. (e) Photomicrograph showing the boxed region from panel d, where the collateral branches from the main axon just below the central canal. (f) Aligned reconstruction of a lamina I IN with a compact slightly asymmetrical axon, dominating the lateral side of the cell. (g) Lamina I IN with a sparser, more symmetrical axon centered on the soma. Note that in both cases (f, g), the axon occupies mostly laminae I–II. (h) Reconstruction of a laterally positioned IN with a recurrent axon that fills also the medial aspect of the DH. (i) Photomicrograph showing a dorsally spanning lower order collateral that branches from a higher order axon in a perpendicular, candle-like manner. Note that for all aligned reconstructions, the spinal cord, gray matter, and central canal contours were taken from the section that contains the soma; therefore, some of the processes in distant sections may appear to fall outside the boundaries of the contours. The irregularity of the contours is due to faithful representation of the section contours after the shrinkage and distortions that occurred during histological processing. Arrow, axon collateral in PNs/lower order branch in INs; arrowhead, main axon in PNs/higher order branch in INs; dashed line, gray matter border toward dorsal funiculus. Scale bars: 250 μm in the reconstructions; 50 μm in panel e; 100 μm in panel i. Soma and dendrites are in blue, and axon is orange in all the reconstructions.

had a clear collateral bearing varicosities that passed through lamina X and also aimed toward dorsal laminae (Figure 1d,e). However, the main axon in this case gave rise to this collateral on the contralateral side.

INs analyzed in this study showed axonal trees similar to those of our earlier reconstructions from sagittal sections (Szucs et al., 2013). The transverse sectioning plane in this case, however, allowed a clear distinction of two major variations of the axonal trees. The first and more frequent IN axon type (10 out of 15) was a compact dense axon that did not exceed significantly (Figure 1f) or stayed within (Figure 1g) the mediolateral span of the dendrites of the neuron. In either case, the axonal tree was centered on the soma and appeared to have little or no asymmetry. The axon branches of this tree type were concentrated in laminae I–II with only occasional protrusions in deeper laminae. Another, less frequent axonal tree type (five out of 15) was a sparser axon that innervated regions that fell well outside the mediolateral area occupied by the dendrites (Figure 1h,i), usually toward the medial direction resulting in great asymmetry. An extreme variation of this morphology was already reported in our earlier work (see figure 4 in Szucs et al., 2013). This type of axon always showed the candelabra-like collateral branching (Szucs et al., 2013) when a higher order axon branch running between laminae III and IV gave rise to collaterals branching in an almost perpendicular manner and running toward the superficial laminae where they arborized extensively. Axon collaterals of both PNs and INs could be detected outside the boundaries of the gray matter, frequently in the dorsolateral funiculus and occasionally in the dorsal funiculus.

3.2 | Relative spatial distribution of dendritic and axonal trees

Thin and thick primary afferents carrying electrical signals of different sensory modalities show heterogeneity in their entry sites and distribution along the mediolateral axis of the superficial DH. Since both axonal and dendritic trees of the reconstructed neurons showed variable mediolateral asymmetry, we checked if there is any correlation between the asymmetry of the dendritic and axonal trees in the

mediolateral and rostrocaudal directions. The method of determining symmetry of the dendritic and axonal trees is visually explained in Figure 2a,b (see the figure legend for detailed explanation of the calculation). While dendritic trees of PNs and INs showed similar variation in their mediolateral symmetry, the axons of INs were more centered on the soma, while PN collaterals were located significantly more lateral to the soma (Figure 2c). Along the rostrocaudal axis, PNs and INs showed a similarly large variability of the side where the axonal and dendritic dominance occurred (Figure 2d). Axon collaterals and dendrites of PNs showed a clear tendency (78%) to be distributed on the same side of the soma (termed as homologous distribution; Figure 2e), while contrary to this, the majority of INs (80%) had a heterologous distribution, that is, their axons and dendrites dominated the opposite side of the soma. Interestingly, PNs showed a mostly heterologous distribution (78%) along the rostrocaudal axis (Figure 2f), while the IN group had almost equal cases of homologous (47%) and heterologous (53%) distribution of the processes. We also checked if the somatodendritic type or firing pattern of the neuron showed any correlation with the distribution type of the axons or dendrites. Most likely due to the modest sample size, we could not detect correlation between these parameters (Figure 3).

It is well established that both lamina I PNs and INs frequently possess axon-bearing dendrites (Szucs et al., 2010, 2013). Thus, we quantified the percentage of axon and dendrites in four spatial quadrants (rostromedial, rostrolateral, caudomedial, and caudolateral) around the neuronal somata to see if the location of the axon-bearing dendrite shows any correlation with the distribution of the axon around the cell. In line with the symmetry analyses in Figure 2, PN processes were more polarized (very dark and very pale spatial quadrants; Figure 4b–d), while IN processes were more equally distributed around the soma (Figure 4e–g). In case of neurons with axon-bearing dendrites, axon collaterals of PNs and axonal processes of INs were mostly concentrated in quadrants other than the one containing the dendrite that gave rise to the axon (Figure 4b,e). We were also unable to reveal any typical distribution pattern correlating with the firing pattern or somatodendritic type of either PNs (Figure 4c,d) or INs (Figure 4f,g).

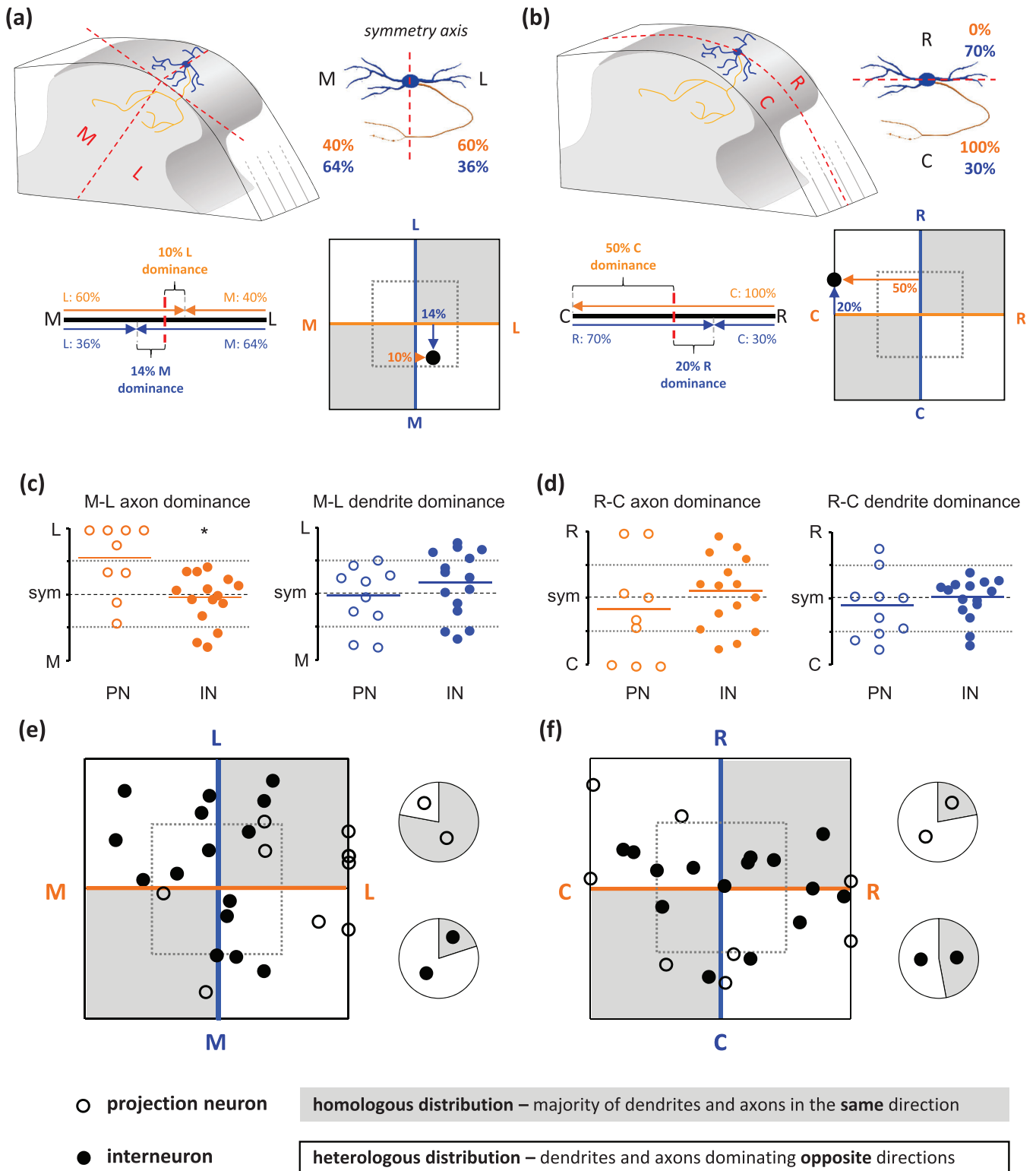


FIGURE 2 Mediolateral and rostrocaudal symmetry of PN and IN processes. (a, b) Schematic drawings explaining spatial distribution analyses of labeled cell processes in the reconstructed and aligned serial sections. (a) For determining mediolateral symmetry of the processes, a dorsoventral guideline was drawn perpendicular to the tangential line touching the dorsal horn (DH) surface at the point where the soma was located. Guidelines are indicated by the red-dashed lines. The same guideline was used in all the aligned serial sections. Processes medial (M) and lateral (L) to the guideline were considered to be on the corresponding side of the soma. The percentage of processes medial and lateral to the soma was then compared to a 50–50% (absolute symmetry) case resulting in a lateral or medial dendrite and axon dominance value. These dominance values were then used as coordinates of the given neuron in the symmetry matrix. A neuron with absolutely symmetric distribution of its dendrites and axon would be located in the center of the symmetry matrix. Cells that fall in gray quadrants of the symmetry matrix have dendrites and axon

(Continues)

FIGURE 2 (Continued)

that show similar distribution (homologous), while cells in the white quadrants have contrasting process distributions (heterologous). The dotted square indicates the -25% to 25% dominance area of the symmetry matrix. (b) Rostrocaudal symmetry was analyzed in the same manner using an imaginary plane (zero level in Z) crossing the largest diameter of the soma. The location of the zero plane in the serial reconstruction is indicated with the dashed red line. (c) Mediolateral axon (orange) and dendrite (blue) dominance values of PNs (hollow circles) and INs (full circles). Axon collaterals of PNs showed a significant lateral dominance compared to axons of INs. (d) Rostrocaudal axon (orange) and dendrite (blue) dominance of PNs (hollow circles) and INs (full circles). While both axon collaterals and dendrites of PNs showed a wider distribution, there were no significant differences of the means compared to similar processes of INs. (e) Mediolateral symmetry matrix of PNs (hollow circles) and INs (full circles). Majority (78%) of PNs showed homologous distribution of axon collaterals and dendritic processes, while distribution of IN axonal and dendritic processes was mostly heterologous. (f) Rostrocaudal symmetry matrix of PNs and INs showing mostly (78%) heterologous distribution of PNs and no preference for homologous or heterologous distribution of INs, as roughly half of them fell in either category.

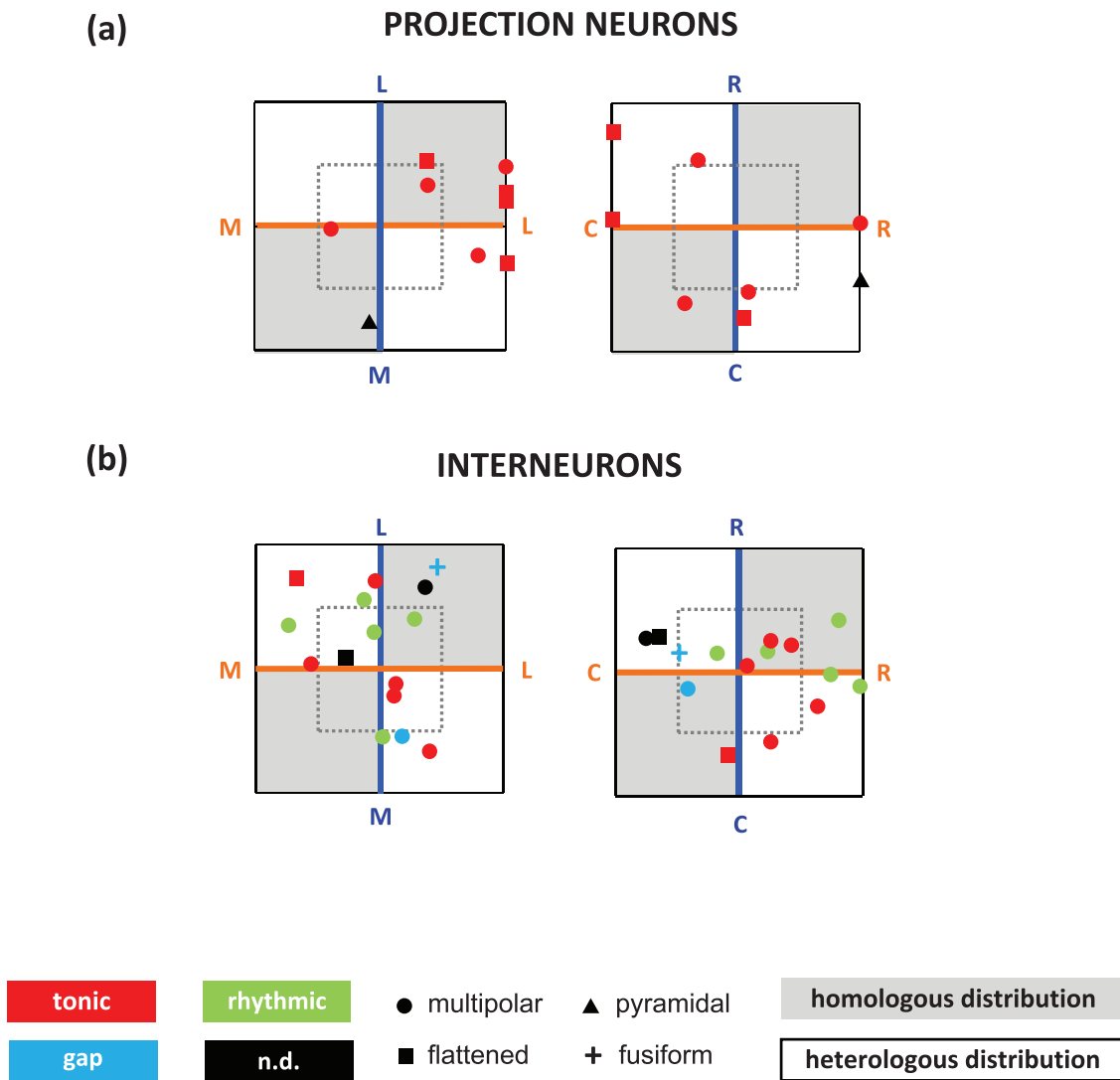


FIGURE 3 Mediolateral (a) and rostrocaudal (b) symmetry matrices of PNs and INs. Each cell is represented by a symbol reflecting its somatodendritic type (Lima & Coimbra, 1986), while the color of the symbol indicates the firing pattern (Luz et al., 2014). None of the investigated features correlated with the symmetry preference.

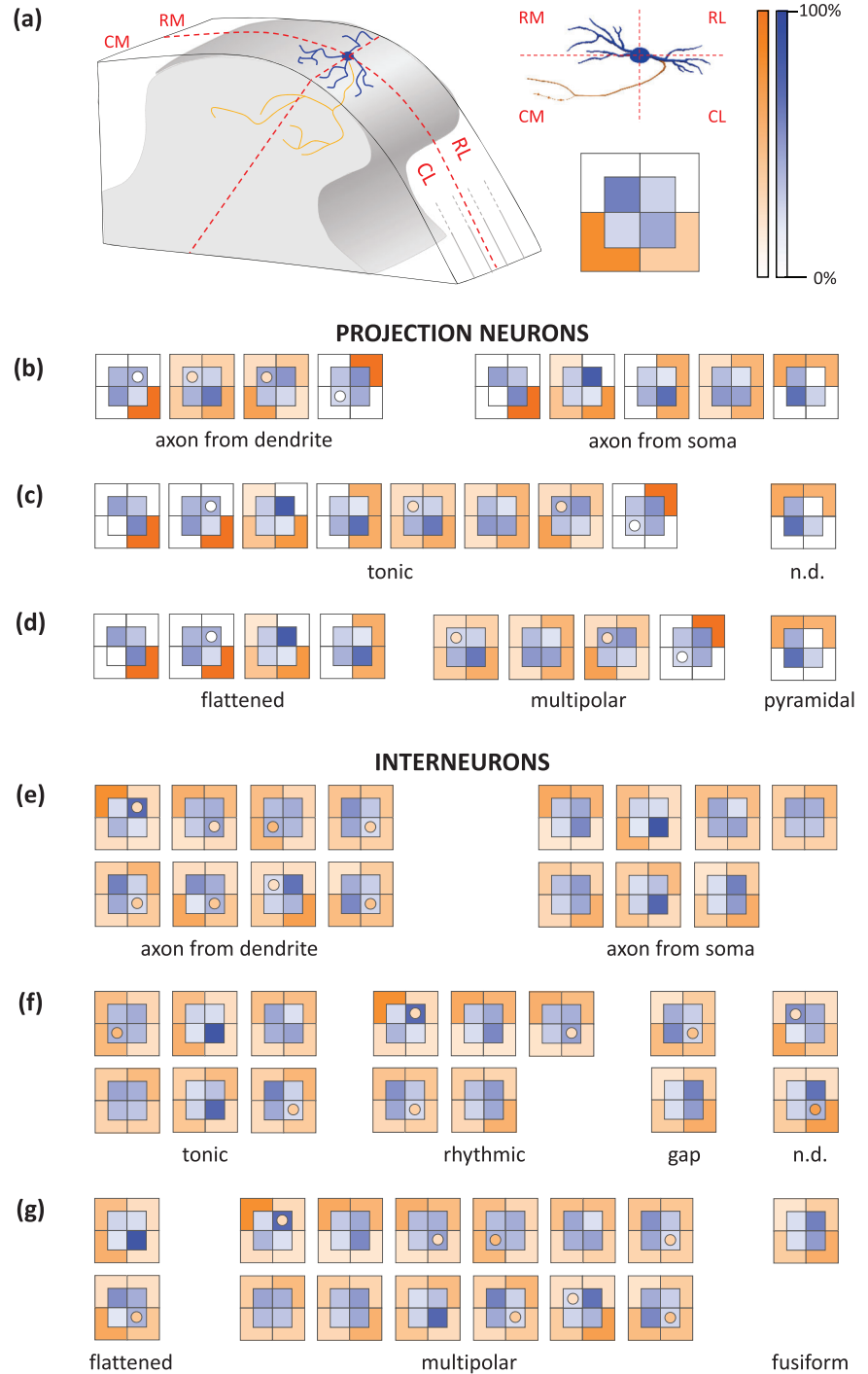
3.3 | Interlaminar distribution of axonal and dendritic processes

As average density of processes in any given lamina can be very much distorted by a single neuron with a dense, extensive process, we also analyzed how frequently each cell group had processes in that lamina

and constructed prevalence maps from these data. High prevalence in a given lamina indicates that that type of neuron (PN or IN) is very likely to have axons/dendrites there.

Dendritic processes of PNs and INs showed very similar distribution among laminae of the spinal cord. As expected, the highest percentage of the mean total length of dendrites was located in

FIGURE 4 For the soma-centered-distribution analysis (a), the rostrocaudal guideline and the zero Z level guiding plane have been used together. The resulting spatial quadrants around the soma are labeled as rostromedial (RM), caudomedial (CM), rostromedial (RL), and caudolateral (CL). Dendrites, blue; axon, orange. Axon and dendrite distribution of the schematic neuron in RM, RL, CM, and CL spatial quadrants. The percentage of axon falling in a given spatial quadrant is indicated by the orange color scale in larger squares, while dendrite distribution is shown in the overlying smaller squares using the blue color scale. (b) PNs with the axon originating from a major dendrite or from the soma. The spatial quadrant where the axon-bearing dendrite resides is indicated by a hole in the blue square. The majority of axon bearing dendrites in PNs are located medial to the soma. (c) Soma-centered distribution of PNs based on their firing pattern reveals that axon-bearing dendrites are more frequent among the multipolar type. (d) Flattened and pyramidal PNs more often showed polarized soma-centered distribution than multipolar PNs. (e) INs with axon-bearing dendrites and ones with (f) regular somatic axon origin. Axon-bearing dendrites were more often located laterally and caudally to the soma. (g) Axon-bearing dendrites were present in INs with all firing types. (c) Similar to PNs, axon-bearing dendrites were more frequent in multipolar INs.



laminae I–II. In line with earlier reports (Lima & Coimbra, 1986; Szucs et al., 2013), almost all PNs and INs in the lateral part of lamina I had dendrites that reached out into the dorsal part of the lateral funiculus (Figure 5a,c). Terminal processes of these dendrites sometimes re-entered the lateral part of laminae III–IV, and INs frequently had ventrally oriented dendrites reaching laminae III–IV. One PN had a medially oriented dendrite that reached the dorsal funiculus; however, this made a negligible contribution to its total dendritic tree and thus did not show up on the bar chart. Similarly, two PNs and a single IN with multipolar somatodendritic morphology had ventrally

oriented dendrites, the terminal part of which descended into lamina V (Figure 5c).

The distribution of the axonal processes showed significant differences in case of PNs and INs. While the largest share of the total axon of all INs fell in lamina II, PNs had the largest percentage of their axon in deeper laminae and in the dorsal part of the LF and only a few had collaterals in lamina II (Figure 5b,d). Occasional axons of both PNs and INs could also be seen in the dorsal funiculus (Figure 5d). All INs had axons in laminae I–IV and more than half of them in lamina V–VI but only less than 10% in lamina VII–X and in the contralateral gray matter.

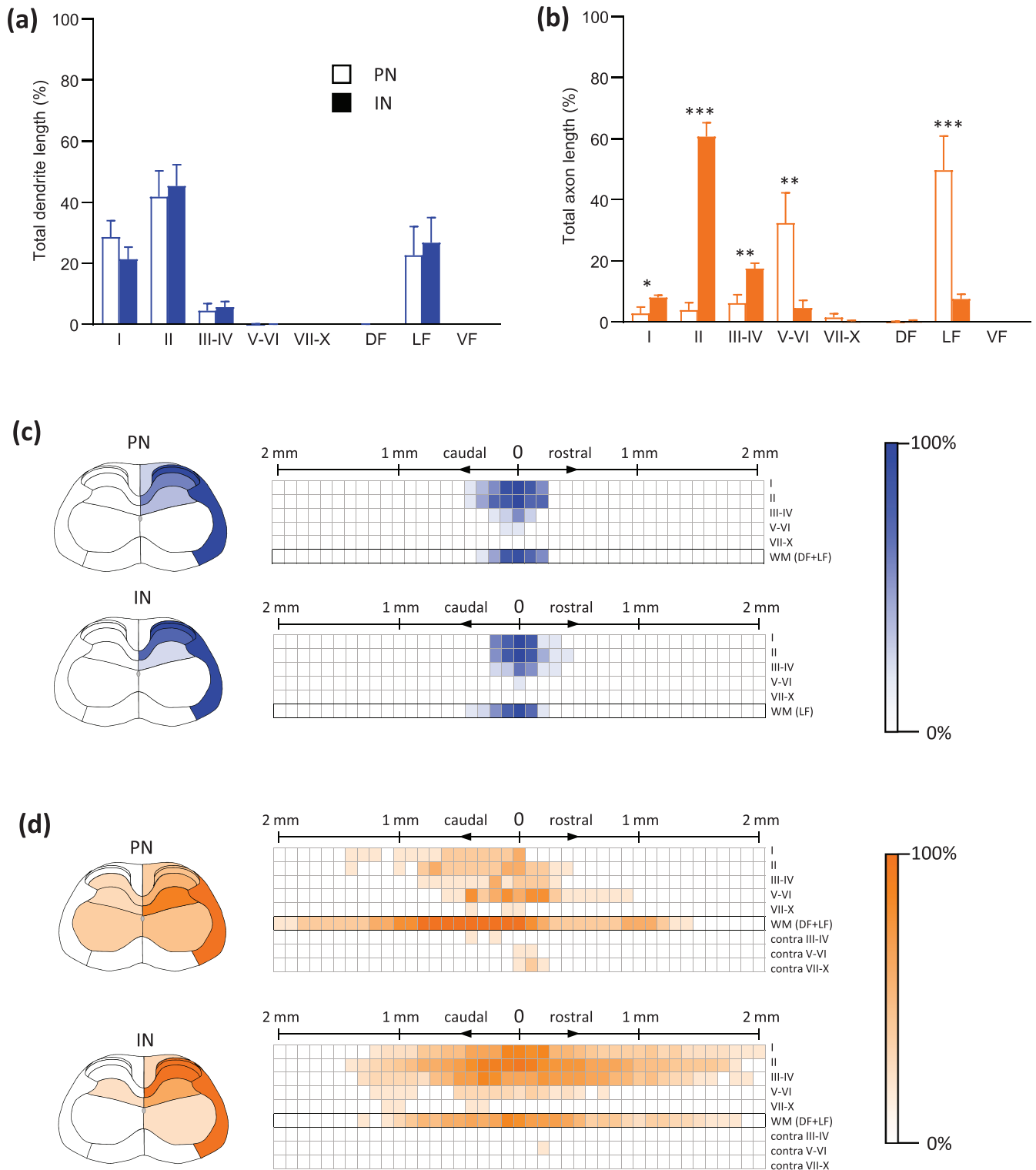


FIGURE 5 Dendrite and axon distribution of PNs and INs in gray matter laminae and white matter funiculi. (a) The mean dendritic length of both PNs and INs was the highest in superficial laminae (I–II) and in the lateral funiculus of the white matter. The distribution pattern of the two groups was almost identical. (b) Mean axon length showed significant differences between the PNs and INs in most parts of the DH and in the lateral funiculus. While laminae II and III–IV contained most parts of the IN axons, the largest portion of PN axon collaterals was located in laminae V–VI and in the lateral funiculus. Mann–Whitney test: * $p < .05$; ** $p < .01$; *** $p < .001$. (c) Dendritic prevalence maps (percentage of neurons with process pieces in the particular region) projected in the transverse plane along the rostrocaudal axis centered on the soma-containing section also show almost identical occurrence of PN and IN dendrites in the investigated laminae. (d) The axon prevalence map projected to the transverse plane and individual prevalences in the serial sections centered to the soma.

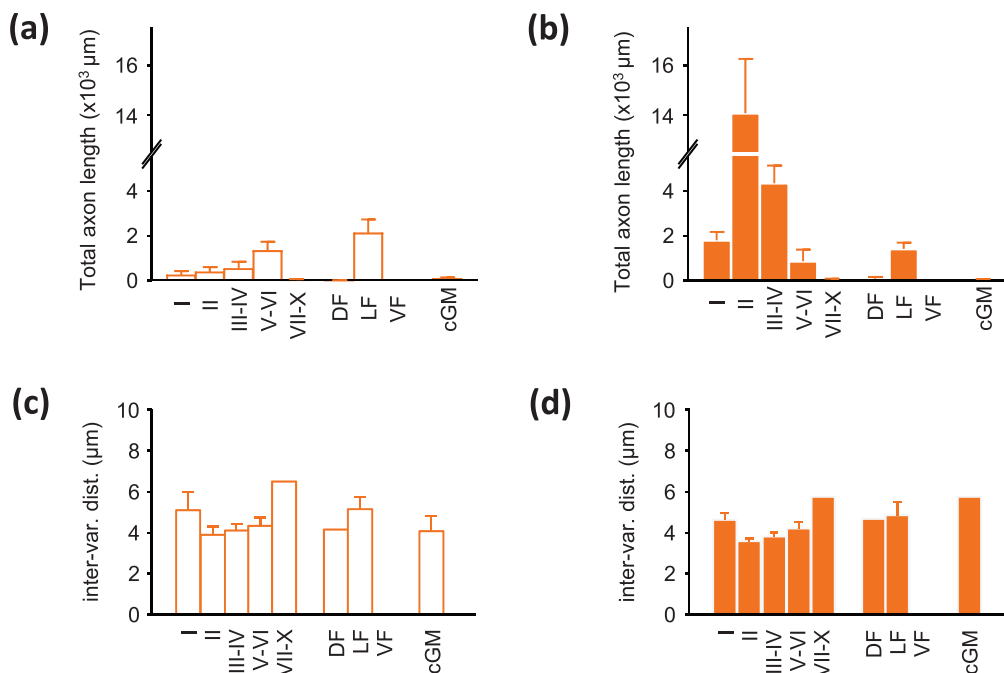


FIGURE 6 Total axon length and average varicosity densities of PN and IN axons. While the total axon length nicely reflected the proportional distributions shown in Figure 5, INs had at least 10 times more axon (a) than PN collaterals (b) in all the investigated gray matter laminae and white matter funiculi. (c, d) The average density of varicosities along IN axons and PN axon collaterals was almost identical in all investigated regions.

PNs had axons less frequently in laminae I–IV; all of them had axons in lamina V–VI and roughly the same prevalence of them in lamina VII–X, as that of IN axons in these laminae. The contralateral laminae III–X received occasional PN collaterals more frequently. Interestingly, PN axons sent collaterals more frequently in the caudal direction, while IN axons more in the rostral direction (Figure 5d). Interestingly, three PNs had local collateral branches that either crossed the midline or branched from the main axon in the contralateral side being in almost all laminae. There was only a single IN that sent its axon collaterals to the contralateral laminae V–VI (Figure 5d).

The total length of the axon collaterals of PNs was one fifth of the total axonal length of INs, but showed a distribution similar to the relative distribution (Figure 6a,b). The density of varicosities along the axon did not show significant differences in any of the regions between PNs and INs (Figure 6c,d).

3.4 | Activation of NK1 receptors leads to increased excitatory drive in the intermediate gray matter

Application of SP (1 μM) on spinal cord slices resulted in an average 2.5-fold increase in the number of spontaneous EPSPs arriving to lamina VII neurons (Figure 7d). Repeated application of SP could evoke a similar, although less robust, increase in the EPSP numbers (Figure 7a,b). The selective NK1 receptor antagonist, SR140333, did not block the EPSP increase at low concentration (10 nM) but abolished the effect of SP when applied at higher (50–200 nM) concentra-

tions. The effect of SR140333 was reversible in some of the cases (not shown). In the presence of TTX (500 nM), blocking action potential generation, SP could not evoke EPSP number increase, excluding the possibility of activation of presynaptic NK1 receptors (He et al., 2019; Matsumura et al., 2021). Finally, when the ipsilateral DH was removed by performing a cut at the base of the DH, application of SP failed to raise the number of EPSPs registered from lamina VII neurons (Figure 7b,c). Thus, ventrally projecting axons of NK1-receptor-expressing superficial DH neurons play a key role in SP-driven excitation of ventral horn neurons. These superficial DH neurons might include PNs that contribute to this excitation, directly or indirectly, via ventral collaterals, but may also involve NK1 receptor expressing INs that can produce indirect activation via other DH neurons (Figure 7e).

4 | DISCUSSION

Axon distribution and trajectory are widely accepted criteria of neuronal classification schemes in several CNS regions, such as the cerebral cortex (DeFelipe et al., 2013; Markram et al., 2015) or hippocampus (Klausberger & Somogyi, 2008; Pelkey et al., 2017). Identification of axonal termination fields and their target domains, based on detailed axonal reconstructions, largely advanced our understanding of the function of microcircuits in several brain regions (Budd et al., 2010; Karube & Kisvarday, 2011; Maccaferri et al., 2000). Furthermore, high-resolution spatial maps and quantitative data derived from single-axon reconstructions provided a novel perspective on several aspects of cortical connectivity (Rockland, 2020). Yet, subcortical

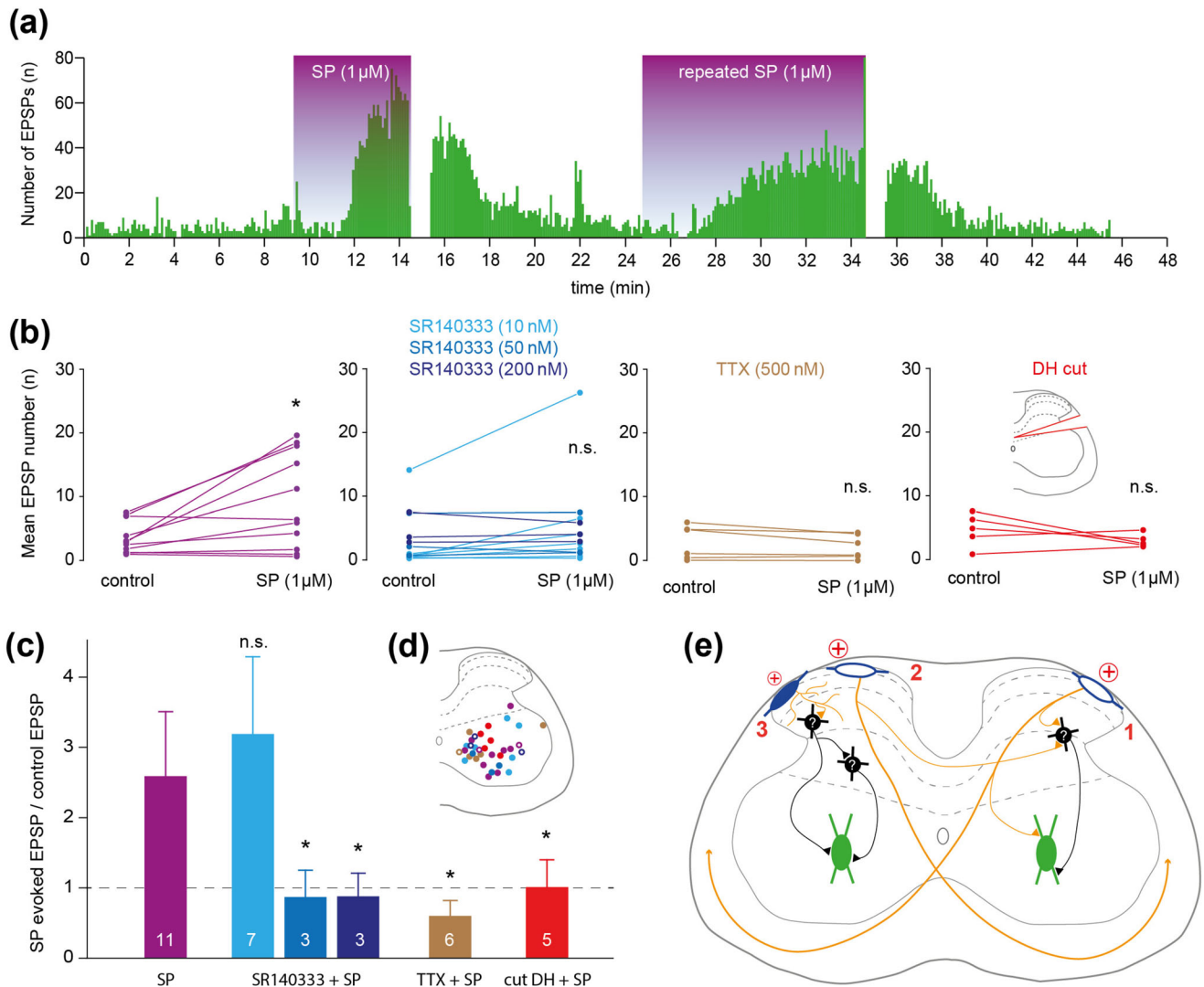


FIGURE 7 Ventrally directed axons of DH NK1 receptor expressing neurons contribute to an excitatory drive onto neurons in ventral laminae. (a) Application of substance P (SP; 1 μ M) in acute spinal cord slices increases the number of spontaneous EPSPs recorded from neurons located in laminae V–VII. Repeated application of SP resulted in a similar but less pronounced increase. (b) The mean EPSP number was significantly increased during application of SP. Although the increase in the mean EPSP number was not fully blocked by a low concentration (10 nM) of the SP antagonist SR140333, the SP-induced modest increase in the EPSP frequency did not reach significance threshold. Higher concentrations of the antagonist (50 nM, 200 nM) blocked the effect of SP. Application of TTX and the mechanical separation of the DH effectively blocked the SP-induced mean EPSP number increase. (c) The average ratio of SP evoked mean EPSP number and control mean EPSP number was significantly reduced (close to 1) in case of effective concentrations of SR140333 (50–200 nM) and TTX (500 nM) or mechanical separation of the DH, as compared to the mean EPSP number ratio (2.59 ± 0.58) for the application of SP alone. Dashed line, ratio = 1; white numbers, numbers of experiments; two-sample Student's *t*-test with Welch correction: **p* < .05. (d) The scheme shows the locations of the recorded neurons, and color code reflects the type of the experiment. Full circles indicate cells that had been recovered, while hollow circles show locations of the cell based on the maps drawn from the slice during the recording. (e) Hypothetical scheme showing how ventral collaterals (orange) of (1) ipsilateral PNs (hollow; blue), (2) commissural collaterals (orange) of contralateral PNs (hollow; blue), and (3) local axons (orange) of INs (filled; blue) may excite neurons in ventral laminae (green) directly or indirectly via one or more putative excitatory INs (black) with unknown location. The red plus signs indicate PNs and INs as putative NK1 receptor-bearing neurons responding to SP application. The size of the red plus sign reflects the probability of SP activation.

areas, often due to technical difficulties, gained much less attention in this respect, leading to rather simplistic circuit descriptions.

While a substantial amount of data is available about the somatodendritic morphology of spinal lamina I neurons (Lima & Coimbra, 1983, 1986, 1988, 1989), the laminar and segmental distribution pattern of their axons is much less characterized. All studies agree that the

percentage of PNs in this lamina is small (Al-Khater et al., 2008; Browne et al., 2021; Todd, 2010) and only a few reports suggested their active participation in sensory processing (Narotzky & Kerr, 1978; Yeziarski et al., 1980) rather than limiting their roles to integrators and output elements of the DH circuitry. Our earlier qualitative descriptions of lamina I PN and IN axons also suggested significant involvement in DH

circuits and indicated substantial differences in the axonal targets of the two groups (Szucs et al., 2010, 2013). Thus, the main goal of this study was to analyze the spatial distribution pattern of the dendritic and axonal processes of spinal lamina I neurons. We used NeuroLucida to fully reconstruct 10 lamina I PNs and 15 INs in 3D. We show that while these PNs and INs have almost identical dendritic input fields, their local axon collateral distribution patterns are distinct. We suggest that INs whose cell bodies reside in lamina I establish connections mostly within the superficial DH and can bridge the medial and lateral halves of the DH. In addition to their supraspinal targets, PNs also relay their input locally, preferably to deeper laminae of the spinal gray matter. Furthermore, both PNs and INs have axonal and dendritic architecture that would allow them to be linked propriospinally.

4.1 | Technical considerations

There are some limitations that have to be considered when interpreting results of the present study. First of all, using the intact spinal cord preparation biased our sample to the more accessible lateral part of the DH. Also, due to the very challenging character of serial reconstructions, our sample is limited for both PNs and INs. This fact did not allow us to reveal possible correlations between our symmetry/distribution data and neuronal populations defined on the basis of somatodendritic, electrophysiological, or neurochemical properties. Also, our PNs were not retrogradely labeled from supraspinal target areas but were identified on the basis of a single main axon reaching the contralateral anterolateral white matter, and therefore could be considered as “putative PNs.” However, based on our previous papers and experience with single-cell reconstructions, we are confident that our PN sample included only supraspinally projecting lamina I neurons. It should also be noted that retrograde labeling may also cause bias for certain subsets of lamina I PNs depending on the accuracy of the injection, quality of transport, and so forth. The post hoc identification approach allowed us to work with the whole neuronal population of lateral lamina I. Another limitation arose from our sectioning plane, since the numerous short pieces of processes in the sequential transverse sections could not be readily connected to complete axonal and dendritic trees. This, however, was not critical for the kind of quantitative analyses used in the present study.

Last but not least, animals used in this study are very young and the age groups used for the morphology and slice electrophysiology experiment differ slightly. These animals are still within the first 2 weeks of postnatal development and the circuitry at this point is not yet fully mature. We think, however, that the results derived from the electrophysiology data are not undermined by these changes of the circuitry. The dorsal-to-ventral projections of PNs are unlikely to disappear as we observed ventral collaterals of PNs also in older rats. The neuronal circuitry involved in polysynaptic dorsal-to-ventral connections might change indeed, as GABA and glycine contribution increases, but that is unlikely to affect the putative direct excitatory connections that can be formed via ventral collaterals.

4.2 | Segmental contralateral projection of lamina I PN axon collaterals

In addition to our previous description of lamina I PN collaterals, reconstructions from transverse sections provided evidence that axon collaterals can also cross the midline in the dorsal commissure or branch from the main axon on the contralateral side. Although our sample of PNs is moderate, one third of the reconstructed axons had contralateral collaterals, while out of the 15 lamina I INs only a single had an axon collateral crossing the midline. The former collateral type might have been among the axons reported to cross the midline in the dorsal commissure after biotinylated dextran amine (BDA) injection into the lateral part of lamina III and IV (Petko & Antal, 2000), where the main axon of this type of lamina I PN passes through. The axon varicosities found on this type of collateral and also on the one observed to branch from the main axon on the contralateral side may represent synapses formed on lamina X neurons, virtually all of which integrate mono- and polysynaptic inputs from several types of thin primary afferent fibers and play an important role in nociception (Krotov et al., 2019). Since ventral collaterals of lamina I PNs also innervate the ipsilateral lamina V, it is reasonable to suggest that, via their collaterals, lamina I PNs might recruit or modulate other supraspinally projecting cell populations and link ascending systems.

4.3 | Dendritic and axonal distribution patterns and functional asymmetry of the superficial DH

Neurons in lamina I belong to the late-born population of DH neurons. While early-born dorsal neurons migrate mostly ventrolaterally and find their final location in deeper laminae of the DH, the late-born population migrates dorsolaterally and occupies the superficial layers of the DH (Chen, 2019). These postmitotic neurons extend their neurites as they migrate; as they disperse tangentially in the thin band of lamina I, in close contact with TrkA+ sensory afferents (Roome et al., 2022), they are likely to encounter spatial limitations that might determine the final arrangement of their dendrites and axon. The proximity of the dorsal pial surface and the high density of primary afferents in the dorsal root entry zone allow growth of the processes only in the ventral direction. As a consequence, dorsoventral asymmetry is a characteristic feature of certain types of lamina I neurons and ventrally oriented dendrites have been demonstrated for both lamina I PNs and INs (Kosugi et al., 2013; Lima & Coimbra, 1986; Szucs et al., 2013). The presence or absence of ventral dendrites defines two distinct classes of lamina I cells receiving input from primary afferent fibers having different central termination fields and processing different modalities (Kosugi et al., 2013).

Although the mediolateral and rostrocaudal growth of lamina I neuron processes is less restricted, similar anatomical constraints may also exist in these directions. The dense bundles of thick primary afferents entering the medial part of the dorsal root entry zone may also form a physical obstacle for the growing processes of lamina I neurons. Indeed,

both anatomical and functional mediolateral asymmetry of lamina I neurons had been reported earlier (Kosugi et al., 2013; Mizuno et al., 2019). Excitatory input zones of lamina I neurons, defined by laser-scanning photostimulation, showed a marked medial asymmetry that matched the structural asymmetry of the dendritic fields of the neurons (Kosugi et al., 2013). A later work from the same group concluded that the difference between lateral and medial DH in responsiveness for focal electrical stimulation results from properties of intrinsic elements of the DH, such as the direction of local connectivity. Their hypothesis was that neurons in the most medial part of the superficial DH tend to make excitatory synaptic connections preferentially onto neurons that are lateral to their cell body and this might reverse direction for neurons at more central location (Mizuno et al., 2019). This hypothesis fits well our finding that lamina I INs in the lateral part of the DH present heterologous axonal and dendritic distribution.

The axons of some lamina I neurons were shown to issue varicosity-bearing collaterals that generate arbors that overlap the neurons' dendritic territories in lamina I (Bennett et al., 1981). In our present sample, the majority of lamina I INs had axons that surrounded the dendritic arbor of the neurons. However, one third of lamina I INs had axons extending all the way to the medial end of the DH while leaving most of their dendrites in the most lateral aspect of the DH. This axon configuration was also demonstrated in sagittal sections (Szucs et al., 2013). Mediolateral projections from the lateral and medial end of the deep DH had been reported earlier (Petko & Antal, 2000) in rats, although suspected to originate from deep DH laminae. A recent work analyzing irradiating pain syndromes in the lumbar region and certain headaches suggested that there might be specific DH neurons that bridge lateral and medial primary afferent entry zones and serve as the anatomical basis for irradiating pain and lateromedial information spread (Defrin et al., 2020). The medially spanning axon phenotype of lamina I INs described in the present work seems to provide evidence for this hypothesis. The axon of lamina I INs can spread information along the mediolateral axis and our finding that most INs showed heterologous axon/dendrite distribution also supports this notion. One cannot exclude that the most polarized neurons having medial axons and dendrites with very lateral location are the extreme examples of lateromedial information transmitters. This also raises the possibility that medially located INs might possess axons reaching the most lateral parts of the DH or even the lateral white matter. Such hypothetical neurons, however, did not occur in our sample, due to the fact that our imaging technique gives better access to the lateral half of the DH (Szucs et al., 2009) and therefore our sample had a bias to lateral lamina I neurons. While it would be important to connect this phenotype to the known classifications based on the presence of neurochemical markers (Gatto et al., 2019; Todd, 2017) or genetic background (Haring et al., 2018) of DH neurons, most of the recent data had been accumulated in mice and not in rat. The lack of correlation between somatodendritic type or firing pattern with our investigated parameters (symmetry in process distribution) does not go against earlier findings that link different functions to somatodendritic types among lamina I PNs. It rather means that the spatial distribution of the axon and dendrites of lamina I neurons might be yet another parameter to consider when their

diversity is assessed. These quantitative spatial differences might better correlate with somatotopy, integrative properties, or other, yet unidentified functional differences.

4.4 | PN collaterals provide excitatory drive to laminae V–VII and might contribute to the nociceptive flexor reflex directly

Information flow from deeper to superficial laminae in normal and pathological conditions has been demonstrated by recent works using transgenic technologies to target selected populations of DH INs (Braz et al., 2014; Cordero-Erausquin et al., 2016; Duan et al., 2014; Francois et al., 2017; Petitjean et al., 2015). Classical (Melzack & Wall, 1965) and all recent gating theories of pain transmission consider INs in laminae II–III (Cordero-Erausquin et al., 2016) as the anatomical substrate of interactions between primary afferent inputs of different modalities but overlook the role of lamina I neurons. A recent review, however, suggested that placing PNs via their axon collaterals, as new players in spinal cord pain processing, might help refine the connectivity principles in the spinal nociceptive network and might eventually explain some of its still ambiguous actions (Browne et al., 2020). The authors of this review also point out that “feedforward” excitation and “feedback” inhibition through inhibitory INs are both probable functions of PN collaterals. The sole evidence for “feedforward” excitation of neighboring PNs comes from an *in vitro* recording experiment from a pair of synaptically connected lamina I PNs (Luz et al., 2010). Here, we present evidence for SP-evoked “feedforward” excitatory drive onto lamina VII neurons, some of which are last-order premotor INs that relay the sensory activation to motoneurons, forming a pathway that might be part of the withdrawal reflex. The premotor apparatus, however, is not the only candidate for receiving this relayed information. Wide dynamic range neurons in deeper laminae might also be among targets of ventral axon collaterals of lamina I PNs, relaying nociceptive input for their integrated output toward supraspinal centers. Neurons giving rise to the spinocerebellar tracts can be among the targets as well as autonomic sympathetic preganglionic neurons at the thoracolumbar segments in the lateral horn.

Neurokinin 1 receptors (NK1R) are expressed on ~45% of lamina I neurons (Todd et al., 1998), majority of which is likely to be excitatory (Littlewood et al., 1995). Around 80% of PNs express NK1R (Al-Khater et al., 2008; Marshall et al., 1996; Todd et al., 2000) and despite the fact that INs were shown to have weak NK1R staining (Al Ghamdi et al., 2009; Cheunsuang & Morris, 2000), one third of them responded to SP application, although this response was smaller than that in PNs (Luz et al., 2014). The time course of the depolarization caused by bath application of SP (see figure 7 in Luz et al. (2014)) suggests a significant difference in functional NK1 receptor expression between INs and PNs. Our result that only higher concentrations of the NK1 receptor antagonist could block the SP-induced excitatory drive indicates that the contribution of lamina I INs (weaker NK1 receptor expression) is probably a lot smaller than those of PNs that are known to be rich in NK1 receptors. Thus, we hypothesize that both INs and PNs in lamina I responding to SP might contribute to linking the anterolateral

ascending system to other ascending pathways, or the premotor apparatus within the ventral horn forming an anatomical basis for the nociceptive withdrawal reflex. The observation that mechanical separation of the DH prevents the SP-evoked excitatory drive strongly supports our hypothesis. However, based on our morphological data, the dominance of IN axons in superficial laminae suggests access to other INs involved in mostly sensory networks and, through these, an indirect influence on deeper laminae. PN axon collaterals, on the other hand, are more abundant in deeper laminae where they have better access to INs involved in motor networks, and to motoneuron dendrites, on which they might even directly form synapses. Nevertheless, since this hypothesis is mostly based on our morphological data, further experiments will be needed to differentiate the contribution of INs and PNs to the dorsal-to-ventral information flow.

5 | CONCLUSION

In summary, lamina I neurons have distinct local axon collateral distribution patterns that imply their diverse roles in the spinal cord circuitry. INs, with their heterologous axonal and dendritic distribution along the mediolateral axis, provide an anatomical substrate for the functional asymmetries in the superficial DH and for the mediolateral information flow explaining observations of radiating pain. At the same time, INs indirectly, and PNs possibly directly, via axon collaterals projecting to deeper laminae, mediate a dorsoventral excitatory drive that can establish a link between the anterolateral system and several other spinal sensory, autonomic, and motor processing pathways.

AUTHOR CONTRIBUTIONS

Lilana L. Luz and Elisabete C. Fernandes performed the recordings and filled the neurons in semi-intact spinal cords. Éva Kókai reconstructed the neurons, designed and performed the analyses, and drafted the manuscript. Pierrick Poisbeau designed and analyzed the slice electrophysiology experiments. Peter Szucs performed the patch clamp recordings in slice preparations, analyzed the data, and wrote the manuscript. Boris V. Safronov wrote the manuscript.

ACKNOWLEDGMENTS

This project was supported by the Hungarian Brain Research Program (KTIA_NAP_13-2-2014-0005 to E.K., P.S.; 2017-1.2.1-NKP-2017-00002 to E.K. and P.S.), and the Marie-Curie Short Term Fellowship (P.S.). P.P. is a senior fellow of the Institut Universitaire de France and receives support from the Graduate School of Pain (EURIDOL, ANR-17-EURE-022). The authors would like to thank Prof. Andrew J. Todd for critical reading of the manuscript.

CONFLICT OF INTEREST

The authors declare no conflict of interest.

DATA AVAILABILITY STATEMENT

The data that support the findings of this study are available from the corresponding author upon reasonable request.

ORCID

Peter Szucs  <https://orcid.org/0000-0003-4635-6427>

REFERENCES

- Al-Khater, K. M., Kerr, R., & Todd, A. J. (2008). A quantitative study of spinothalamic neurons in laminae I, III, and IV in lumbar and cervical segments of the rat spinal cord. *Journal of Comparative Neurology*, 511(1), 1–18. <https://doi.org/10.1002/cne.21811>
- Al Ghamdi, K. S., Polgar, E., & Todd, A. J. (2009). Soma size distinguishes projection neurons from neurokinin 1 receptor-expressing interneurons in lamina I of the rat lumbar spinal dorsal horn. *Neuroscience*, 164(4), 1794–1804. <https://doi.org/10.1016/j.neuroscience.2009.09.071>
- Beal, J. A., Penny, J. E., & Bicknell, H. R. (1981). Structural diversity of marginal (lamina I) neurons in the adult monkey (*Macaca mulatta*) lumbosacral spinal cord: A Golgi study. *Journal of Comparative Neurology*, 202(2), 237–254. <https://doi.org/10.1002/cne.902020209>
- Bennett, G. J., Abdelmoumene, M., Hayashi, H., Hoffert, M. J., & Dubner, R. (1981). Spinal cord layer I neurons with axon collaterals that generate local arbors. *Brain Research*, 209(2), 421–426. [https://doi.org/10.1016/0006-8993\(81\)90164-5](https://doi.org/10.1016/0006-8993(81)90164-5)
- Braz, J., Solorzano, C., Wang, X., & Basbaum, A. I. (2014). Transmitting pain and itch messages: A contemporary view of the spinal cord circuits that generate gate control. *Neuron*, 82(3), 522–536. <https://doi.org/10.1016/j.neuron.2014.01.018>
- Brown, A. G. (1981). *Organization in the spinal Cord: The anatomy and physiology of identified neurones*. Springer-Verlag.
- Browne, T. J., Hughes, D. I., Days, C. V., Callister, R. J., & Graham, B. A. (2020). Projection neuron axon collaterals in the dorsal horn: Placing a new player in spinal cord pain processing. *Front Physiol*, 11, 560802. <https://doi.org/10.3389/fphys.2020.560802>
- Browne, T. J., Smith, K. M., Gradwell, M. A., Iredale, J. A., Days, C. V., Callister, R. J., Hughes, D. I., & Graham, B. A. (2021). Spinoparabrachial projection neurons form distinct classes in the mouse dorsal horn. *Pain*, 162(7), 1977–1994. <https://doi.org/10.1097/j.pain.0000000000002194>
- Budd, J. M., Kovacs, K., Ferecsko, A. S., Buzas, P., Eysel, U. T., & Kisvarday, Z. F. (2010). Neocortical axon arbors trade-off material and conduction delay conservation. *Plos Computational Biology*, 6(3), e1000711. <https://doi.org/10.1371/journal.pcbi.1000711>
- Cervero, F., & Iggo, A. (1980). The substantia gelatinosa of the spinal cord: A critical review. *Brain*, 103(4), 717–772. <https://doi.org/10.1093/brain/103.4.717>
- Chen, Z. (2019). Common cues wire the spinal cord: Axon guidance molecules in spinal neuron migration. *Seminars in cell & developmental biology*, 85, 71–77. <https://doi.org/10.1016/j.semcdb.2017.12.012>
- Cheunsuang, O., & Morris, R. (2000). Spinal lamina I neurons that express neurokinin 1 receptors: Morphological analysis. *Neuroscience*, 97(2), 335–345. [https://doi.org/10.1016/s0306-4522\(00\)00035-x](https://doi.org/10.1016/s0306-4522(00)00035-x)
- Cordero-Erausquin, M., Inquimbert, P., Schlichter, R., & Hugel, S. (2016). Neuronal networks and nociceptive processing in the dorsal horn of the spinal cord. *Neuroscience*, 338, 230–247. <https://doi.org/10.1016/j.neuroscience.2016.08.048>
- DeFelipe, J., Lopez-Cruz, P. L., Benavides-Piccione, R., Bielza, C., Larranaga, P., Anderson, S., Burkhalter, A., Cauli, B., Fairén, A., Feldmeyer, D., Fishell, G., Fitzpatrick, D., Freund, T. F., González-Burgos, G., Hestrin, S., Hill, S., Hof, P. R., Huang, J., Jones, E. G., ... Ascoli, G. A. (2013). New insights into the classification and nomenclature of cortical GABAergic interneurons. *Nature Reviews Neuroscience*, 14(3), 202–216. <https://doi.org/10.1038/nrn3444>
- Defrin, R., Brill, S., Goor-Arieh, I., Wood, I., & Devor, M. (2020). "Shooting pain" in lumbar radiculopathy and trigeminal neuralgia, and ideas concerning its neural substrates. *Pain*, 161(2), 308–318. <https://doi.org/10.1097/j.pain.0000000000001729>

- Duan, B., Cheng, L., Bourane, S., Britz, O., Padilla, C., Garcia-Campmany, L., Krashes, M., Knowlton, W., Velasquez, T., Ren, X., Ross, S., Lowell, B. B., Wang, Y., Goulding, M., & Ma, Q. (2014). Identification of spinal circuits transmitting and gating mechanical pain. *Cell*, 159(6), 1417–1432. <https://doi.org/10.1016/j.cell.2014.11.003>
- Fernandes, E. C., Santos, I. C., Kokai, E., Luz, L. L., Szucs, P., & Safronov, B. V. (2018). Low- and high-threshold primary afferent inputs to spinal lamina III antenna-type neurons. *Pain*, 159(11), 2214–2222. <https://doi.org/10.1097/j.pain.0000000000001320>
- Fitzgerald, M. (1989). The course and termination of primary afferent fibers. In Wall, P. D. & Melzak, R. (Eds.), *Textbook of pain* (pp. 46–62). Churchill Livingstone.
- Francois, A., Low, S. A., Sypek, E. I., Christensen, A. J., Sotoudeh, C., Beier, K. T., Ramakrishnan, C., Ritola, K. D., Sharif-Naeini, R., Deisseroth, K., Delp, S. L., Malenka, R. C., Luo, L., Hantman, A. W., & Scherrer, G. (2017). A brainstem-spinal cord inhibitory circuit for mechanical pain modulation by GABA and enkephalins. *Neuron*, 93(4), 822.e6–839.e6. <https://doi.org/10.1016/j.neuron.2017.01.008>
- Fyffe, R. E. W. (1984). Afferent fibers. In Davidoff, R. A. (Ed.), *Handbook of the spinal cord* (pp. 79–136). Dekker.
- Gatto, G., Smith, K. M., Ross, S. E., & Goulding, M. (2019). Neuronal diversity in the somatosensory system: Bridging the gap between cell type and function. *Current Opinion in Neurobiology*, 56, 167–174. <https://doi.org/10.1016/j.conb.2019.03.002>
- Gobel, S. (1978). Golgi studies of the neurons in layer I of the dorsal horn of the medulla (trigeminal nucleus caudalis). *Journal of Comparative Neurology*, 180(2), 375–393. <https://doi.org/10.1002/cne.901800212>
- Gradwell, M. A., Boyle, K. A., Browne, T. J., Bell, A. M., Leonardo, J., Peralta Reyes, F. S., Dickie, A. C., Smith, K. M., Callister, R. J., Days, C. V., Hughes, D. I., & Graham, B. A. (2022). Diversity of inhibitory and excitatory parvalbumin interneuron circuits in the dorsal horn. *Pain*, 163(3), e432–e452. <https://doi.org/10.1097/j.pain.0000000000002422>
- Gutierrez-Mecinas, M., Polgar, E., Bell, A. M., Herau, M., & Todd, A. J. (2018). Substance P-expressing excitatory interneurons in the mouse superficial dorsal horn provide a propriospinal input to the lateral spinal nucleus. *Brain Struct Funct*, 223(5), 2377–2392. <https://doi.org/10.1007/s00429-018-1629-x>
- Haring, M., Zeisel, A., Hochgerner, H., Rinwa, P., Jakobsson, J. E. T., Lonnerberg, P., La Manno, G., Sharma, N., Borgius, L., Kiehn, O., Lagerström, M. C., Linnarsson, S., & Ernfrors, P. (2018). Neuronal atlas of the dorsal horn defines its architecture and links sensory input to transcriptional cell types. *Nature Neuroscience*, 21(6), 869–880. <https://doi.org/10.1038/s41593-018-0141-1>
- He, Z. X., Liu, T. Y., Yin, Y. Y., Song, H. F., & Zhu, X. J. (2019). Substance P plays a critical role in synaptic transmission in striatal neurons. *Biochemical and Biophysical Research Communications*, 511(2), 369–373. <https://doi.org/10.1016/j.bbrc.2019.02.055>
- Karube, F., & Kisvarday, Z. F. (2011). Axon topography of layer IV spiny cells to orientation map in the cat primary visual cortex (area 18). *Cerebral Cortex*, 21(6), 1443–1458. <https://doi.org/10.1093/cercor/bhq232>
- Klausberger, T., & Somogyi, P. (2008). Neuronal diversity and temporal dynamics: The unity of hippocampal circuit operations. *Science*, 321(5885), 53–57. <https://doi.org/10.1126/science.1149381>
- Kosugi, M., Kato, G., Lukashov, S., Pendse, G., Puskar, Z., Kozsurek, M., & Strassman, A. M. (2013). Subpopulation-specific patterns of intrinsic connectivity in mouse superficial dorsal horn as revealed by laser scanning photostimulation. *Journal of Physiology*, 591(7), 1935–1949. <https://doi.org/10.1113/jphysiol.2012.244210>
- Krotov, V., Tokhtamysh, A., Safronov, B. V., Belan, P., & Voitenko, N. (2019). High-threshold primary afferent supply of spinal lamina X neurons. *Pain*, 160(9), 1982–1988. <https://doi.org/10.1097/j.pain.0000000000001586>
- Lima, D. (1998). Anatomical basis for the dynamic processing of nociceptive input. *European Journal of Pain (London, England)*, 2(3), 195–202. [https://doi.org/10.1016/s1090-3801\(98\)90015-5](https://doi.org/10.1016/s1090-3801(98)90015-5)
- Lima, D., & Coimbra, A. (1983). The neuronal population of the marginal zone (lamina I) of the rat spinal cord. A study based on reconstructions of serially sectioned cells. *Anat Embryol*, 167(2), 273–288.
- Lima, D., & Coimbra, A. (1986). A Golgi study of the neuronal population of the marginal zone (lamina I) of the rat spinal cord. *Journal of Comparative Neurology*, 244(1), 53–71. <https://doi.org/10.1002/cne.902440105>
- Lima, D., & Coimbra, A. (1988). The spinothalamic system of the rat: Structural types of retrogradely labelled neurons in the marginal zone (lamina I). *Neuroscience*, 27(1), 215–230.
- Lima, D., & Coimbra, A. (1989). Morphological types of spinomesencephalic neurons in the marginal zone (lamina I) of the rat spinal cord, as shown after retrograde labelling with cholera toxin subunit B. *Journal of Comparative Neurology*, 279(2), 327–339. <https://doi.org/10.1002/cne.902790212>
- Littlewood, N. K., Todd, A. J., Spike, R. C., Watt, C., & Shehab, S. A. (1995). The types of neuron in spinal dorsal horn which possess neurokinin-1 receptors. *Neuroscience*, 66(3), 597–608. [https://doi.org/10.1016/0306-4522\(95\)00039-1](https://doi.org/10.1016/0306-4522(95)00039-1)
- Lu, Y., & Perl, E. R. (2003). A specific inhibitory pathway between substantia gelatinosa neurons receiving direct C-fiber input. *Journal of Neuroscience*, 23(25), 8752–8758.
- Lu, Y., & Perl, E. R. (2005). Modular organization of excitatory circuits between neurons of the spinal superficial dorsal horn (laminae I and II). *Journal of Neuroscience*, 25(15), 3900–3907. <https://doi.org/10.1523/JNEUROSCI.0102-05.2005>
- Luz, L. L., Szucs, P., Pinho, R., & Safronov, B. V. (2010). Monosynaptic excitatory inputs to spinal lamina I anterolateral-tract-projecting neurons from neighbouring lamina I neurons. *Journal of Physiology*, 588(Pt 22), 4489–4505. <https://doi.org/10.1113/jphysiol.2010.197012>
- Luz, L. L., Szucs, P., & Safronov, B. V. (2014). Peripherally driven low-threshold inhibitory inputs to lamina I local-circuit and projection neurons: A new circuit for gating pain responses. *Journal of Physiology*, 592(7), 1519–1534. <https://doi.org/10.1113/jphysiol.2013.269472>
- Maccaferri, G., Roberts, J. D., Szucs, P., Cottingham, C. A., & Somogyi, P. (2000). Cell surface domain specific postsynaptic currents evoked by identified GABAergic neurones in rat hippocampus in vitro. *Journal of Physiology*, 524(Pt 1), 91–116. <https://doi.org/10.1111/j.1469-7793.2000.t01-3-00091.x>
- Markam, H., Muller, E., Ramaswamy, S., Reimann, M. W., Abdallah, M., Sanchez, C. A., Ailamaki, A., Alonso-Nanclares, L., Antille, N., Arsever, S., Kahou, G. A., Berger, T. K., Bilgili, A., Buncic, N., Chalmourda, A., Chindemi, G., Courcol, J. D., Delalondre, F., Delattre, V., ... Schurmann, F. (2015). Reconstruction and simulation of neocortical microcircuitry. *Cell*, 163(2), 456–492. <https://doi.org/10.1016/j.cell.2015.09.029>
- Marshall, G. E., Shehab, S. A., Spike, R. C., & Todd, A. J. (1996). Neurokinin-1 receptors on lumbar spinothalamic neurons in the rat. *Neuroscience*, 72(1), 255–263. [https://doi.org/10.1016/0306-4522\(95\)00558-7](https://doi.org/10.1016/0306-4522(95)00558-7)
- Matsumura, S., Yamamoto, K., Nakaya, Y., O'Hashi, K., Kaneko, K., Takei, H., Tsuda, H., Shirakawa, T., & Kobayashi, M. (2021). Presynaptic NK1 receptor activation by substance P suppresses EPSCs via nitric oxide synthesis in the rat insular cortex. *Neuroscience*, 455, 151–164. <https://doi.org/10.1016/j.neuroscience.2020.12.012>
- Melzack, R., & Wall, P. D. (1965). Pain mechanisms: A new theory. *Science*, 150(3699), 971–979. <https://doi.org/10.1126/science.150.3699.971>
- Mizuno, M., Kato, G., & Strassman, A. M. (2019). Spatial organization of activity evoked by focal stimulation within the rat spinal dorsal horn as visualized by voltage-sensitive dye imaging in the slice. *Journal of Neurophysiology*, 122(4), 1697–1707. <https://doi.org/10.1152/jn.00697.2018>
- Narotzky, R. A., & Kerr, F. W. (1978). Marginal neurons of the spinal cord: Types, afferent synaptology and functional considerations. *Brain Research*, 139(1), 1–20. [https://doi.org/10.1016/0006-8993\(78\)90056-2](https://doi.org/10.1016/0006-8993(78)90056-2)
- Oury-Donat, F., Lefevre, I. A., Thurneyssen, O., Gauthier, T., Bordey, A., Feltz, P., Emonds-Alt, X., Le Fur, G., & Soubrie, P. (1994). SR 140333, a

- novel, selective, and potent nonpeptide antagonist of the NK1 tachykinin receptor: Characterization on the U373MG cell line. *Journal of Neurochemistry*, 62(4), 1399–1407. <https://doi.org/10.1046/j.1471-4159.1994.62041399.x>
- Paxinos, G. W. C. (2007). *The rat brain in stereotaxic coordinates* (6th ed.). Elsevier.
- Pelkey, K. A., Chittajallu, R., Craig, M. T., Tricoire, L., Wester, J. C., & McBain, C. J. (2017). Hippocampal GABAergic Inhibitory Interneurons. *Physiological Reviews*, 97(4), 1619–1747. <https://doi.org/10.1152/physrev.00007.2017>
- Petitjean, H., Pawlowski, S. A., Fraine, S. L., Sharif, B., Hamad, D., Fatima, T., Berg, J., Brown, C. M., Jan, L. Y., Ribeiro-da-Silva, A., Braz, J. M., Basbaum, A. I., & Sharif-Naeini, R. (2015). Dorsal horn parvalbumin neurons are gate-keepers of touch-evoked pain after nerve injury. *Cell reports*, 13(6), 1246–1257. <https://doi.org/10.1016/j.celrep.2015.09.080>
- Petko, M., & Antal, M. (2000). Propriospinal afferent and efferent connections of the lateral and medial areas of the dorsal horn (laminae I–IV) in the rat lumbar spinal cord. *Journal of Comparative Neurology*, 422(2), 312–325. [https://doi.org/10.1002/\(SICI\)1096-9861\(20000626\)422:2312::AID-CNE1130.CO;2-A](https://doi.org/10.1002/(SICI)1096-9861(20000626)422:2312::AID-CNE1130.CO;2-A)
- Ramon y Cajal, S. (1909). *Histologie du Systeme Nerveux de l'homme et des Vertebres*. A. Maloine.
- Ranson, S. W. (1913). The course within the spinal cord of the non-medullated fibers of the dorsal roots: A study of Lissauer's tract in the cat. *Journal of Comparative Neurology*, 23(4), 259–281.
- Rethelyi, M. (1984). Synaptic connectivity in the spinal dorsal horn. In Davidoff, R. A. (Ed.), *Handbook of the spinal cord* (pp. 137–175). Dekker.
- Rexed, B. (1952). The cytoarchitectonic organization of the spinal cord in the cat. *Journal of Comparative Neurology*, 96(3), 415–495.
- Rockland, K. S. (2020). What we can learn from the complex architecture of single axons. *Brain Struct Funct*, 225(4), 1327–1347. <https://doi.org/10.1007/s00429-019-02023-3>
- Roome, R. B., Rastegar-Pouyani, S., Ker, A., Dumouchel, A., Kmita, M., & Kania, A. (2022). Netrin1 and reelin signaling are required for the migration of anterolateral system neurons in the embryonic spinal cord. *Pain*, 163(4), e527–e539. <https://doi.org/10.1097/j.pain.0000000000002444>
- Santos, S. F., Rebelo, S., Derkach, V. A., & Safronov, B. V. (2007). Excitatory interneurons dominate sensory processing in the spinal substantia gelatinosa of rat. *Journal of Physiology*, 581(Pt 1), 241–254. <https://doi.org/10.1113/jphysiol.2006.126912>
- Schoenen, J. (1982). The dendritic organization of the human spinal cord: The dorsal horn. *Neuroscience*, 7(9), 2057–2087. [https://doi.org/10.1016/0306-4522\(82\)90120-8](https://doi.org/10.1016/0306-4522(82)90120-8)
- Smith, K. M., Browne, T. J., Davis, O. C., Coyle, A., Boyle, K. A., Watanabe, M., Dickinson, S. A., Iredale, J. A., Gradwell, M. A., Jobling, P., Callister, R. J., Dayas, C. V., Hughes, D. I., & Graham, B. A. (2019). Calretinin positive neurons form an excitatory amplifier network in the spinal cord dorsal horn. *Elife*, 8, e49190. <https://doi.org/10.7554/eLife.49190>
- Szucs, P., Luz, L. L., Lima, D., & Safronov, B. V. (2010). Local axon collaterals of lamina I projection neurons in the spinal cord of young rats. *Journal of Comparative Neurology*, 518(14), 2645–2665. <https://doi.org/10.1002/cne.22391>
- Szucs, P., Luz, L. L., Pinho, R., Aguiar, P., Antal, Z., Tiong, S. Y., Todd, A. J., & Safronov, B. V. (2013). Axon diversity of lamina I local-circuit neurons in the lumbar spinal cord. *Journal of Comparative Neurology*, 521(12), 2719–2741. <https://doi.org/10.1002/cne.23311>
- Szucs, P., Pinto, V., & Safronov, B. V. (2009). Advanced technique of infrared LED imaging of unstained cells and intracellular structures in isolated spinal cord, brainstem, ganglia and cerebellum. *Journal of Neuroscience Methods*, 177(2), 369–380. <https://doi.org/10.1016/j.jneumeth.2008.10.024>
- Todd, A. J. (2010). Neuronal circuitry for pain processing in the dorsal horn. *Nature Reviews Neuroscience*, 11(12), 823–836. <https://doi.org/10.1038/nrn2947>
- Todd, A. J. (2017). Identifying functional populations among the interneurons in laminae I–III of the spinal dorsal horn. *Mol Pain*, 13, 1744806917693003. <https://doi.org/10.1177/1744806917693003>
- Todd, A. J., McGill, M. M., & Shehab, S. A. (2000). Neurokinin 1 receptor expression by neurons in laminae I, III and IV of the rat spinal dorsal horn that project to the brainstem. *European Journal of Neuroscience*, 12(2), 689–700. <https://doi.org/10.1046/j.1460-9568.2000.00950.x>
- Todd, A. J., Spike, R. C., & Polgar, E. (1998). A quantitative study of neurons which express neurokinin-1 or somatostatin sst2a receptor in rat spinal dorsal horn. *Neuroscience*, 85(2), 459–473. [https://doi.org/10.1016/s0306-4522\(97\)00669-6](https://doi.org/10.1016/s0306-4522(97)00669-6)
- Yasaka, T., Tiong, S. Y. X., Hughes, D. I., Riddell, J. S., & Todd, A. J. (2010). Populations of inhibitory and excitatory interneurons in lamina II of the adult rat spinal dorsal horn revealed by a combined electrophysiological and anatomical approach. *Pain*, 151(2), 475–488. <https://doi.org/10.1016/j.pain.2010.08.008>
- Yezielski, R. P., Culberson, J. L., & Brown, P. B. (1980). Cells of origin of propriospinal connections to cat lumbosacral gray as determined with horseradish peroxidase. *Experimental Neurology*, 69(3), 493–512.
- Yu, X. H., Zhang, E. T., Craig, A. D., Shigemoto, R., Ribeiro-da-Silva, A., & De Koninck, Y. (1999). NK-1 receptor immunoreactivity in distinct morphological types of lamina I neurons of the primate spinal cord. *Journal of Neuroscience*, 19(9), 3545–3555.
- Zhang, E. T., & Craig, A. D. (1997). Morphology and distribution of spinothalamic lamina I neurons in the monkey. *Journal of Neuroscience*, 17(9), 3274–3284.
- Zhang, E. T., Han, Z. S., & Craig, A. D. (1996). Morphological classes of spinothalamic lamina I neurons in the cat. *J Comp Neurol*, 367(4), 537–549. [https://doi.org/10.1002/\(SICI\)1096-9861\(19960415\)367:4537::AID-CNE530.CO;2-5](https://doi.org/10.1002/(SICI)1096-9861(19960415)367:4537::AID-CNE530.CO;2-5)
- Zheng, J., Lu, Y., & Perl, E. R. (2010). Inhibitory neurones of the spinal substantia gelatinosa mediate interaction of signals from primary afferents. *J Physiol*, 588(Pt 12), 2065–2075. <https://doi.org/10.1113/jphysiol.2010.188052>

How to cite this article: Kókai, É., Luz, L. L., Fernandes, E. C., Safronov, B. V., Poisbeau, P., & Szucs, P. (2022). Quantitative spatial analysis reveals that the local axons of lamina I projection neurons and interneurons exhibit distributions that predict distinct roles in spinal sensory processing. *Journal of Comparative Neurology*, 530, 3270–3287. <https://doi.org/10.1002/cne.25413>